Wind Energ. Sci. Discuss., doi:10.5194/wes-2016-60, 2017
Manuscript under review for journal Wind Energ. Sci.
Published: 3 February 2017

eawe european academy of wind energy
Open Access WIND ENERGY SCIENCE DISCUSSIONS

An analysis of offshore wind farm SCADA measurements to identify key parameters influencing the magnitude of wake effects

Niko Mittelmeier[1], Julian Allin[1], Tomas Blodau[1], Davide Trabucchi[2], Gerald Steinfeld[2], Andreas Rott[2] and Martin Kühn[2]

[1] Senvion GmbH, Überseering 10, 22297 Hamburg, Germany
[2] ForWind – University of Oldenburg, Institute of Physics, Küpkersweg 70, 26129 Oldenburg

Correspondence to: Niko Mittelmeier (niko.mittelmeier@senvion.com)

Abstract. Atmospheric conditions have a clear influence on wake effects. Stability classification is usually based on wind speed, turbulence intensity, shear and temperature gradients measured partly at met masts, buoys or LiDARs. The objective of this paper is to find a classification for stability based on wind turbine Supervisory Control and Data Acquisition (SCADA) measurements in order to fit engineering wake models better to the current ambient conditions. Two offshore wind farms with met masts have been used to establish a correlation between met mast stability classification and new aggregated artificial signals. The significance of these new signals on power production is demonstrated for two wind farms with met masts and measurements from a long range LiDAR and validated against data from one further wind farm without a met mast. We found a good correlation between the standard deviation of active power divided by the average power of wind turbines in free flow with the ambient turbulence intensity when the wind turbines were operating in partial load. The proposed signal is very sensitive to increased turbulence due to neighbouring turbines and wind farms even at a distance of more than 38 rotor diameters away. It allows to distinguish between conditions with different magnitude of wake effects.

1 Introduction

Wake effects are one of the largest sources of losses in offshore energy yield assessment. This makes wake modelling very important and much research is ongoing to improve wake model predictions. In the latest offshore CREYAP benchmark exercise (Comparative Resource and Energy Yield Assessment Procedure) wake modelling was found to be the prediction with the highest variation among the participants (Mortensen et al., 2015).

In order to be able to use a wake model for validating the performance of an operating offshore wind farm (Mittelmeier et al., 2016) prediction uncertainties need to be reduced. Atmospheric stability has been identified as being one main driver for the variation in power production under waked conditions (Dörenkämper et al., 2012, Westerhellweg et al., 2014, Iungo and Porté-Agel, 2014) and state of the art engineering wake models for industrial application like Fuga or FarmFlow are able to take stability effects into account (Özdemir et al., 2013, Ott and Nielsen, 2014).

Stability classification is based on measurements from met masts, buoys or is assisted by remote sensing devices such as LiDAR or SoDAR. For offshore use, these devices are very expensive and therefore often not permanently available. In

Wind Energ. Sci. Discuss., doi:10.5194/wes-2016-60, 2017
Manuscript under review for journal Wind Energ. Sci.
Published: 3 February 2017

eawe european academy of wind energy
Open Access WIND ENERGY SCIENCE DISCUSSIONS

several studies, LIDAR's have been used to assess the wind speed recovery behind the turbine and wake models have been tuned to match the measured wind speed (Beck et al., 2014, More and Gallacher, 2014).

The purpose of this paper is to investigate wind farm operational data and establish methods of identifying correlations between SCADA statistics and wind turbine wake behaviour caused by different atmospheric conditions.

2 Wind farms and measurements

For this investigation, we select three offshore wind farms, i.e. alpha ventus, Nordsee Ost and Ormonde. The first two wind farms have a well-equipped met mast and provide high quality measurements of hub height wind speed, wind direction, shear and turbulence intensity.

2.1 alpha ventus

The wind farm alpha ventus (AV) is located about 45 km north of the island of Borkum in the North Sea. It consists of twelve turbines of the 5 MW class with a rotordiameter of 126 m and has been commissioned in April 2010. The six northern turbines have been manufactured by Senvion. The six turbines in the southern part of the wind farm (produced by Adwen) are not considered in our analysis. The FINO1 research met mast is only 3.2 rotor diameters west of turbine AV4.

The layout of alpha ventus (Fig. 1) allows for investigating the wake behaviour in single and double wake conditions for westerly wind directions. No data after the period from 3/2011 to 1/2015 is used, because the installation of the Trianel wind farm in the west is supposed to have changed the environmental conditions of alpha ventus by adding extra turbulence to the inflow.

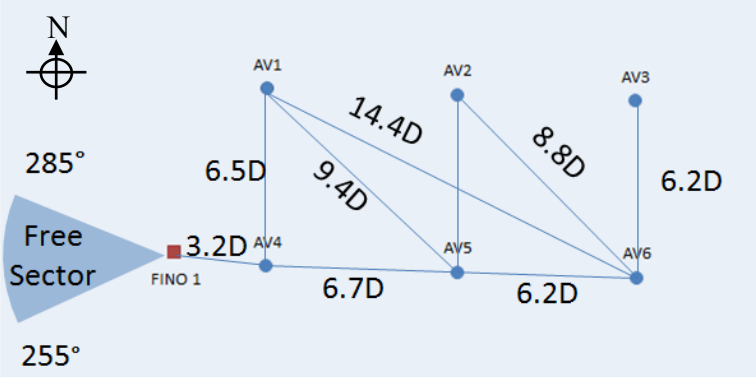

Figure 1: Northern part of alpha ventus and FINO1 met mast layout with free flow sector

Wind Energ. Sci. Discuss., doi:10.5194/wes-2016-60, 2017
Manuscript under review for journal Wind Energ. Sci.
Published: 3 February 2017

eawe european academy of wind energy
Open Access WIND ENERGY SCIENCE DISCUSSIONS

2.2 Nordsee Ost

The wind farm Nordsee Ost (NO) is located about 35 km north-west of the island of Helgoland in the North. The 48 Senvion turbines have a rated power of 6 MW each and a rotor diameter of 126 m. The met mast is located in the south-western corner of the wind farm (Fig. 2). In the south, the neighbouring wind farm Meerwind Ost/Süd reduces the sector of free flow for the met mast as well as the possibilities to study multiple wakes higher than triple wake condition without disturbing effects from Meerwind.

The wind farm Nordsee Ost has been fully commissioned in 2015. So far not enough data (11/2015 – 11/2016) has been collected to investigate the full wake behaviour based on SCADA data. For this reason, a correlation analysis (described in Section 3.2) is performed and the data from the ClusterDesign long range LiDAR measurement campaign is analysed.

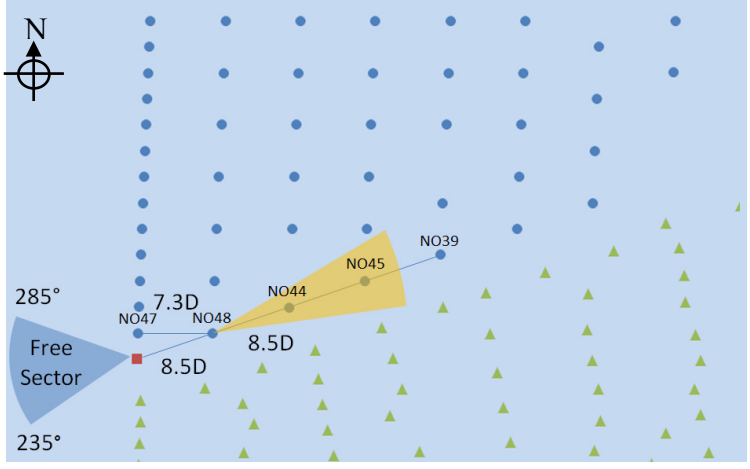

Figure 2: Nordsee Ost (blue cycles) with neighbouring wind farm Meerwind Süd (green triangles) and met mast (red square). Orange area indicates the PPI scan from the Windcube 200S, mounted on the helicopter platform of NO48.

2.3 Ormonde

The Ormonde wind farm consists of 30 Senvion turbines with a rated power of 5 MW and a rotor diameter of 126 m. The wind farm is located in the Irish Sea 10 km west of the Isle of Walney. The selected data is from 1/2012 – 1/2014. During this period, neighbouring wind farms were operational. In the south west, there is Walney 1 (SWT-3.6-107 Siemens) and Walney 2 (SWT-3.6-120 Siemens), in the south there is West of Duddon Sands (SWT-3.6-120 Siemens, fully commissioned 30.10.2014) and in the south east there is Barrow (V90 3.0MW Vestas).

The farm layout displayed in Fig. 3 is structured in a regular array which allows for comparing several multiple-wake situations. The inner farm turbine distance for the investigated wake situation from south west is 6.3 D and from north west is 4.3 D.

Wind Energ. Sci. Discuss., doi:10.5194/wes-2016-60, 2017
Manuscript under review for journal Wind Energ. Sci.
Published: 3 February 2017

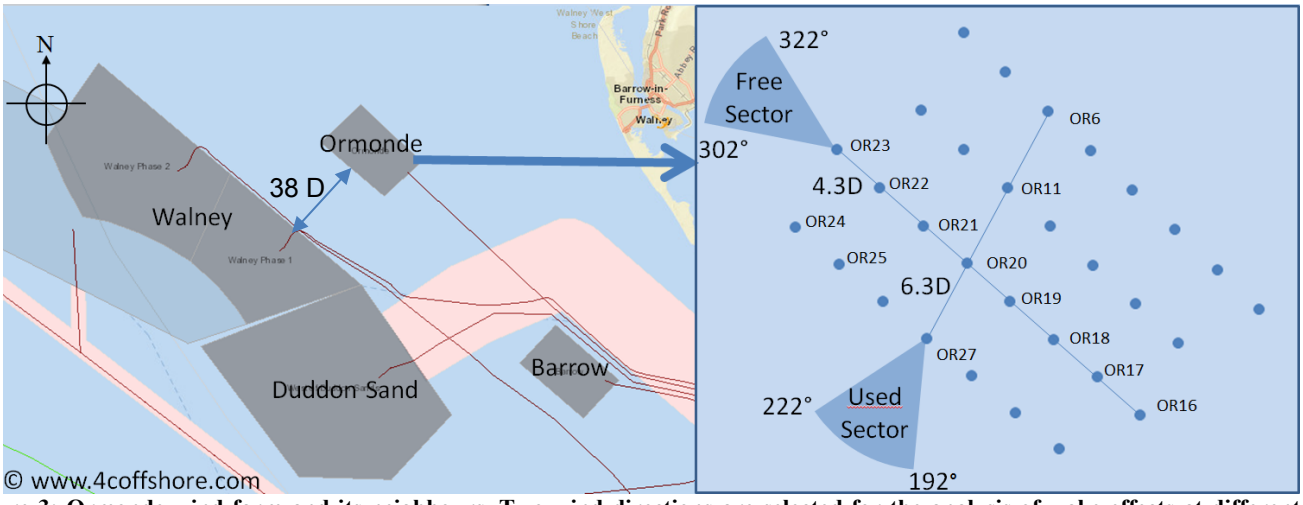

Figure 3: Ormonde wind farm and its neighbours. Two wind directions are selected for the analysis of wake effects at different turbulent classes.

2.4 SCADA and meteorological data

The SCADA data from all wind farms and the meteorological data consist of 10-min statistics. Each turbine provides wind speed, wind direction, active power, yaw position, and pitch angle. The operational condition of the wind turbine which is used for the correlation with the met mast turbulence intensity is categorized by the minimum active power > 10kW, the maximum pitch angle < 3 ° and the standard deviation of the yaw position < 5 °. These filter criteria's ensure that no stand stills, curtailments or too large yaw activities are included in the data. Implausible met mast data is removed and wind directions is corrected for bias by using the orientation of the maximum wake deficit. For the correlation, only sectors of free flow conditions is used.

2.5 Long range LiDAR measurements

Within the "ClusterDesign" research project, funded by the European Union, a long-range LiDAR measurement campaign was realized. A Windcube 200S (WLS200S) LiDAR with scan head was placed on the helicopter platform of NO48 (Fig. 2) from 11/2015 – 5/2016. A differential GPS system composed by three antenna GNSS-System of type Trimble SPS855 / SPS555H allowes for additional measurements of turbines`s yaw and nacelle`s pitch and roll angle. One LiDAR measurement cycle takes about 200 s. It includs five plan position indicator (PPI) scans followed by one range height indicator (RHI) scan. Both scans cover a sector of 30 ° on the horizontal and vertical plane respectively and are centred on the rotor axis. The scan trajectories have an angular resolution of 1 ° and measured the wind speed component along the measuring direction every 25 m from 100 m to 2500 m. The LiDAR data is filtered excluding measurements with a poor signal intensity, or affected by hard targets, or considered outliers.

Wind Energ. Sci. Discuss., doi:10.5194/wes-2016-60, 2017
Manuscript under review for journal Wind Energ. Sci.
Published: 3 February 2017

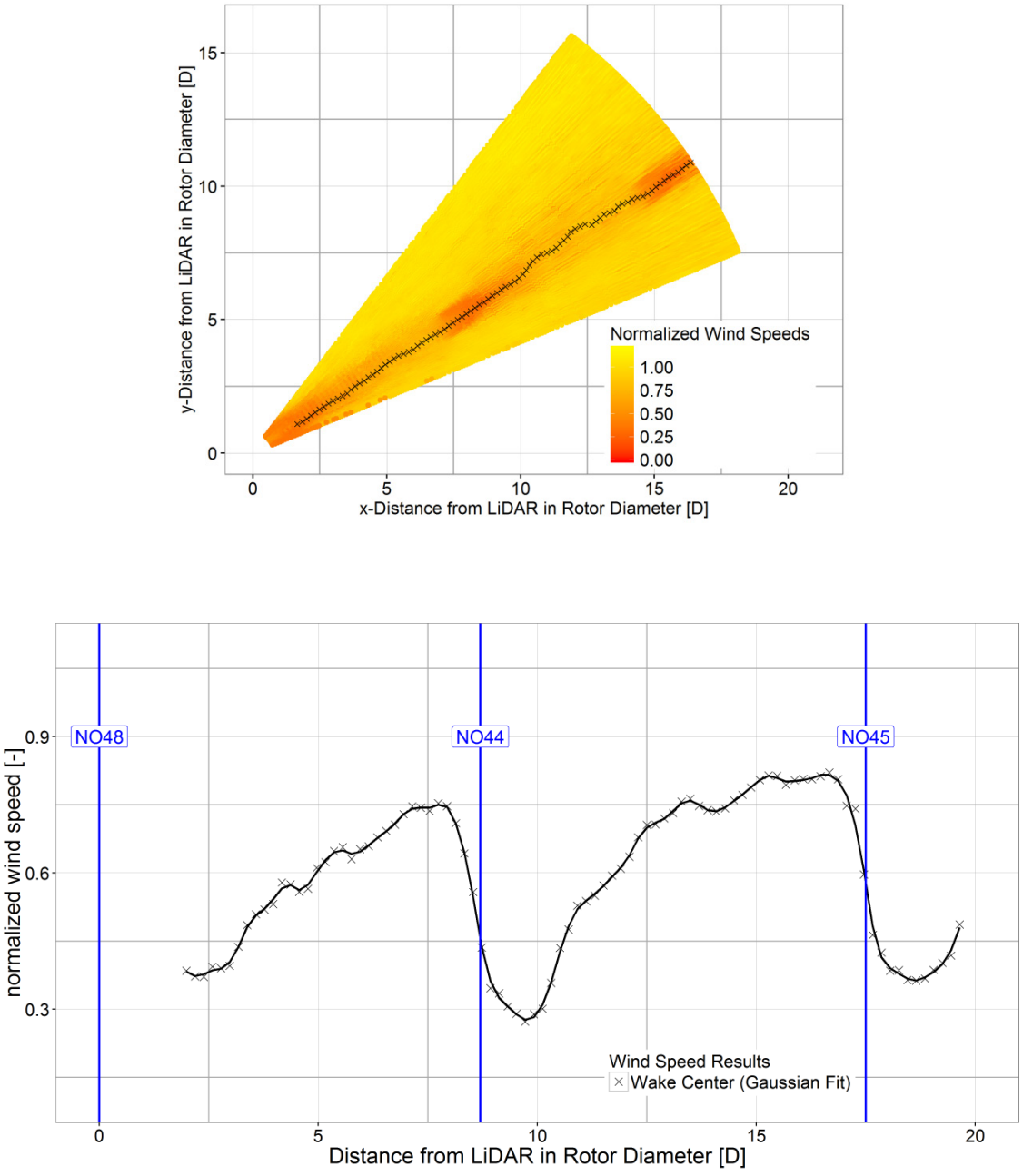

Figure 4: Upper-plot: Visualization of the horizontal plan position indicator (PPI) scans downstream of NO48. Wind speed is normalized with the inflow wind speed, measured at the met mast. The black crosses are the locations of the wind speed minima's derived from a Gaussian fitting for each measurement distance. Bottom-plot: Normalized wind speed as function of the distance in rotor diameters, extracted from the top-plot for the Gaussian fitted minima's (black crosses).

Wind Energ. Sci. Discuss., doi:10.5194/wes-2016-60, 2017
Manuscript under review for journal Wind Energ. Sci.
Published: 3 February 2017

eawe european academy of wind energy
Open Access WIND ENERGY SCIENCE DISCUSSIONS

The horizontal 10-min average wind speed is calculated on a well-defined grid under the assumption of a negligible vertical component of the wind. The average of the wind component measured by the LiDAR during the considered time interval is included in the region of interest of the addressed grid point. The average 10-min wind direction is provided by the met mast. When the latter measurement is not available, the turbine yaw provided by the differential GPS system is used to estimate the wind direction. A detailed description of the LiDAR data pre-processing can be found in Schneemann et al. (2016).

For the assessment in this paper we are using averages of 10-min periods of horizontal wind speed data evaluated from PPI scans of the wake behind NO48. A multiple wake situation can be observed at a wind direction of 236.5 °, when NO45 is in the wake of NO44 and NO48. In Fig. 4 (top) an example for a PPI scan at hub height with averages of 10-min periods of the horizontal wind speed data is displayed. The distance from turbine NO48 is normalised by its rotor diameter and the wind speeds are normalized with the corresponding wind speed measured at the met mast. The different colours represent the wind speed relative to the wind speed at the given met mast location. The black crosses display the locations of the estimated wind speed minima for each measured distance equal or greater than 2 D. These minima are supposed to represent the centre of the wake. They are derived at each downstream cross-section with a Gaussian smoothing (Hamilton, 2015) applied to the LiDAR data before fitting a double-Gaussian-type velocity deficit at the near wake (2 D - 5 D) and a single-Gaussian-type in the far wake. This distinction prevents an overestimation of the deficit in the near wake where the nacelle still has an influence on the flow shape (Keane et al., 2016). The Gaussian minima (black crosses) do not follow a straight line for the entire scan. This should not be interpreted as meandering as we are looking at averages of 10- min periods.
The lower graph of Fig. 4 shows the resulting, normalized wind speeds over the normalized distance from NO48. The black line with the corresponding black crosses refers to the fitted values of the Gaussian fits.

3 Data analysis

3.1. Turbulence, stability and its impact on power production

A stability classification according to the Richardson number expects wind speed and temperature measurements in 10 m and 30 m height. As both met masts fail to fulfil this requirement and as the available temperature measurements have a too large uncertainty to provide reliable stability estimates via the bulk Richardson approach (Saint-Drenan et al., 2009), the simplified classification using turbulence intensity at hub height as proposed by Dörenkämper et al. (2012, 2015) is used for this investigation.
SCADA and LiDAR data is divided into three subsets based on the turbulence intensity from the met mast. Dörenkämper (2015) has suggested a classification into unstable, neutral and stable classes (Table 1). The power production for the different subsets, normalised by free flow power production, is compared for single wake and double wake conditions with data from alpha ventus and FINO1. This kind of analysis reveals the impact only at turbine positions but the wind speed

Wind Energ. Sci. Discuss., doi:10.5194/wes-2016-60, 2017
Manuscript under review for journal Wind Energ. Sci.
Published: 3 February 2017

behaviour in-between turbines is not covered. Therefore at Nordsee Ost, wind speed recovery in single, double and triple wake situations measured by the LiDAR is analysed.

To determine the influence of turbulence and stability on wake effects all available PPIs are analysed and the results of the Gaussian fitted minima's are divided into the same subsets as described in Table 1 based on the turbulence intensity measured at hub height with the met mast.

Table 1: Definition of stratification by met mast turbulence intensity at hub height at alpha ventus and Nordsee Ost

Classification	Turbulence Intensity (TI)
Unstable	TI > 6 %
Neutral	6 % ≥ TI ≥ 4 %
Stable	4 % > TI

3.2 Correlation analysis

At wind farms with no met mast we have to rely on other signals to describe the differences in power production under different atmospheric conditions. To find the best substitute for a met mast measured turbulence intensity several SCADA signals that are affected by turbulence are correlated to the met mast turbulence intensity which is defined as

$$TI_{mast} = \frac{\sigma_{u_{mast}}}{\overline{u_{mast}}} \quad . \tag{1}$$

Analogous to Eq. 1 we define

$$TI_{WT} = \frac{\sigma_{u_{WT}}}{\overline{u_{WT}}} \tag{2}$$

as the turbulence intensity measured with the wind speed anemometer on top of the nacelle with $\bar{u}$ being averages of 10-min periods of horizontal wind speed and its standard deviation σ_u. Göçmen and Giebel (2016) evaluated 1Hz data from Lillgrund and Horns Rev I and found good turbulence estimators by using a turbine derived "WindEstimate" from look-up tables. When only 10-min statistics are available the signals of interest are the standard deviation of the turbine power

$$PO_{std} = \sigma_P, \tag{3}$$

and the normalisation of this signal with the average power $\bar{P}$. This leads to

$$PO_{TI} = \frac{\sigma_P}{\bar{P}}. \tag{4}$$

All SCADA signals can be obtained under free flow conditions or in waked conditions.

3.3 New classification and validation

The new artificial SCADA signal with the highest correlation to the met mast turbulence intensity is used to classify different stratifications. The thresholds are estimated with a two-step approach. First, the power of a turbine in the wake is normalized with the power of a turbine in free flow conditions. This normalized power from a narrow sector of 10° centred at the full wake is divided into three groups. Medium wake effects are ±5 % around the median of the normalized power. High wake effects are 5 % below and low wake effects are 5 % above the median of the normalized power. In the second

Wind Energ. Sci. Discuss., doi:10.5194/wes-2016-60, 2017
Manuscript under review for journal Wind Energ. Sci.
Published: 3 February 2017

step the density distribution of the new SCADA signal is plotted for all three groups and the thresholds are selected to achieve best distinction between the three data sets.

The quality of the established relationship in terms of dependency on turbine type, layout and location of the wind farm is tested by applying the same classification on a different wind farm where no met mast is available.

4 Results and Discussion

4.1 Turbulence stability and its impact on power production

Alpha ventus data from almost four years of operation is used to evaluate the influence of atmospheric stability estimated from the turbulence intensity and its influence on the wake development. Figure 5 proves the different wake behaviour under different turbulence conditions. The top row of plots shows the single wake condition of turbine AV5 in the wake of AV4. The second row displays the same evaluation but for the double wake condition of AV6 in the wake of AV4 and AV5. The left side is a normalised power deficit as function of the wind direction for a wind speed range from 7 m/s to 9 m/s. On the right side, there is the normalised power as function of the wind speed for a sector width of 10 °. Each graph states the total number N of data points which have been split into stable (blue dots), neutral (green diamonds) and unstable (red triangles) data sets. Each symbol is the average of a 2 ° bin (2 m/s bin) and the error bars indicate the standard error of the mean.

For the single wake, a clear distinguishable difference between the stable and unstable power deficit is visible. The largest deviation is found in the full wake. The second wake has a less pronounced difference in power which can be explained by the fact, that the first turbine operating in the wake supports the mixing with the ambient wind speed. Another interesting effect is noticeable in the top left plot. The difference in power for the different stabilities is higher at the right hand side of the deficit in downstream direction. This right drift of the wake in stable conditions has also been observed in LES simulations by Vollmer et al.(2016).

The turbulence intensity for this classification has been measured at 100 m which is the largest height at the FINO1 met mast. The second height of the FINO1 met mast (90 m) is closer to hub height (92 m), but the strong mast structure and the boom orientation of 135 ° causes disturbance for wind directions within the selected sector for our investigation. No further correction, e.g. to account for the difference in height was necessary according to the findings of Tuerk (2008).

For the wind farm Nordsee Ost (NO) only one full year of SCADA data and six month of LiDAR data is available for this investigation. Fifteen PPI scans (as described in Section 2.5) at wind direction from 236 ° - 242 ° are available and categorized according to the classification in Table 1. Fig. 6 displays the wind speed measured with the LiDAR normalized with the inflow wind speed measured at the met mast. The wind speed recovers faster for the unstable turbulence class than for the neutral and stable class. The second and third turbine in the row for the investigated wind direction are marked with blue vertical lines. The decreased wind speed in the induction zone in front of each downstream turbine is clearly visible. The error bars indicate the standard error of the mean. For the stable class $TI \leq 4\%$ only one set of PPI scans is available.

Wind Energ. Sci. Discuss., doi:10.5194/wes-2016-60, 2017
Manuscript under review for journal Wind Energ. Sci.
Published: 3 February 2017

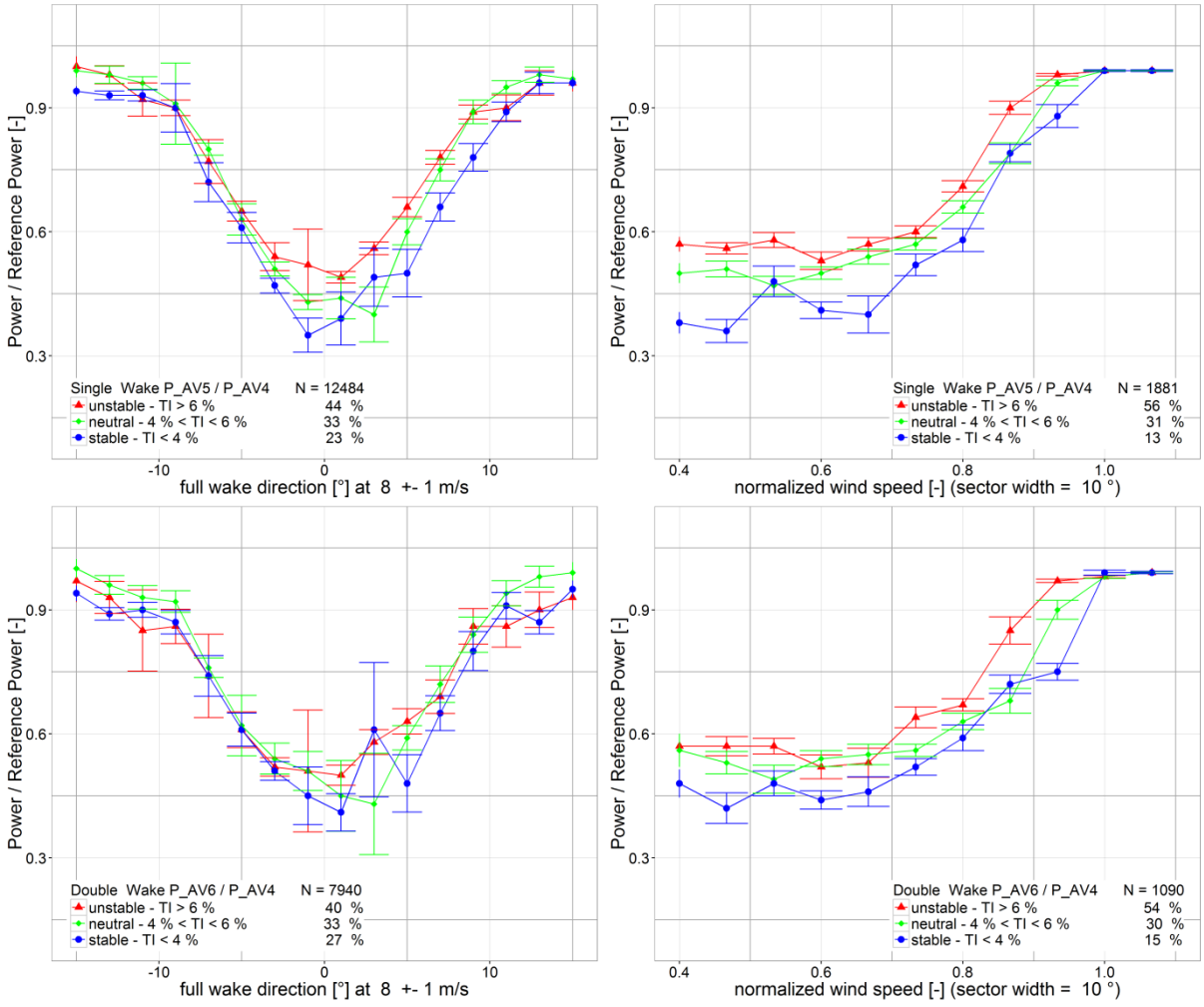

Figure 5: Wake effects in alpha ventus (AV) under different atmospheric conditions classified by met mast turbulence intensity. Power of downstream turbine normalised with free flow turbine. Upper row: single wake, bottom row: double wake. Left column: Normalised Power as function of wind direction, right column: Normalised power as function of wind speed.

Wind Energ. Sci. Discuss., doi:10.5194/wes-2016-60, 2017
Manuscript under review for journal Wind Energ. Sci.
Published: 3 February 2017

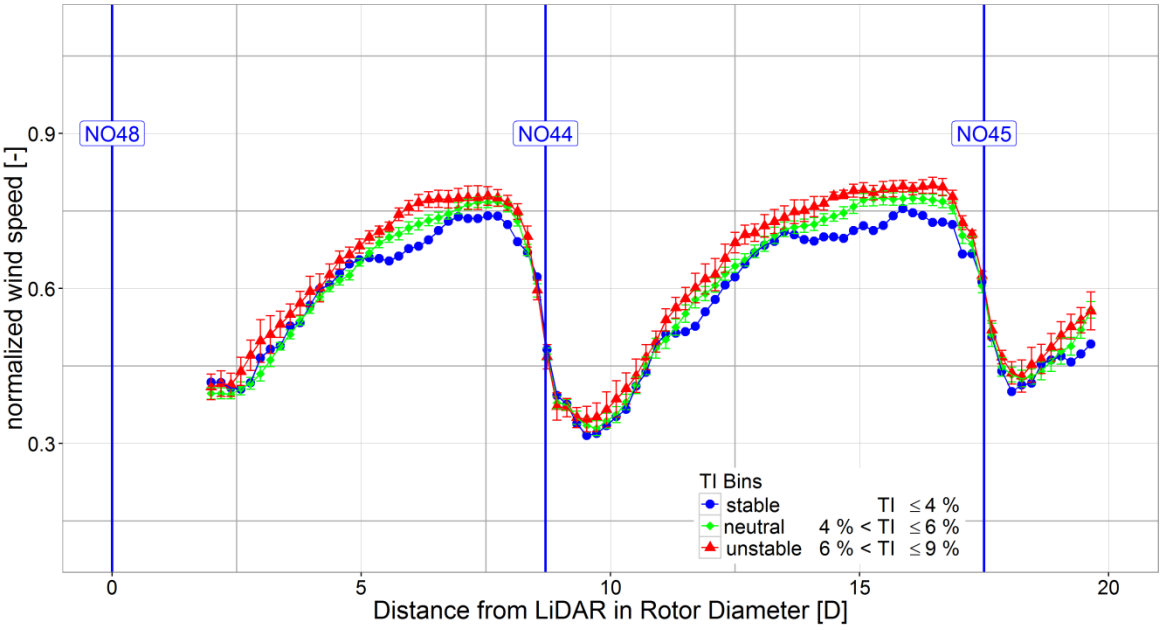

Figure 6: Wind speed recovery at wake centre on hub height behind NO48 for different turbulence stability classes. The wind speed is normalized with the inflow wind speed and the distance from the LiDAR on NO48 downstream is displayed in multiples of rotor diameters

4.2 Correlation analysis

In the next step, we correlate the SCADA signals described in Section 3.2 with the turbulence intensity measured at the mast. In Fig. 7 a panel plot is displayed. The graphs on the diagonal present the histogram and density distribution for the respective variable. The panels above the diagonal provide the Pearson correlation coefficients. The lower panels are scatter plots for the two variables with a fitted linear regression line. The colours of the points indicate the three stability classifications (blue: stable, green: neutral, red: unstable) determined with the met mast turbulence intensity.

The correlation between met mast and turbine TI in subplot (1 , 2) equals to 0.55. This poor result can be explained by the nacelle wind speed measurement position behind the rotor, which induces additional disturbance to the flow.

The highest correlation with the met mast TI is obtained with the standard deviation of the turbine power divided by its average active power ($PO_{TI,AV4}$) in subplot (1 , 5). Although a correlation of 0.66 is not perfect, it is still better than the turbulence measured with the nacelle cup anemometer. Especially in the low turbulence region, the scatter plot proves to be denser. Very similar results are obtained when applying the same analysis to AV1 and AV2.

Wind Energ. Sci. Discuss., doi:10.5194/wes-2016-60, 2017
Manuscript under review for journal Wind Energ. Sci.
Published: 3 February 2017

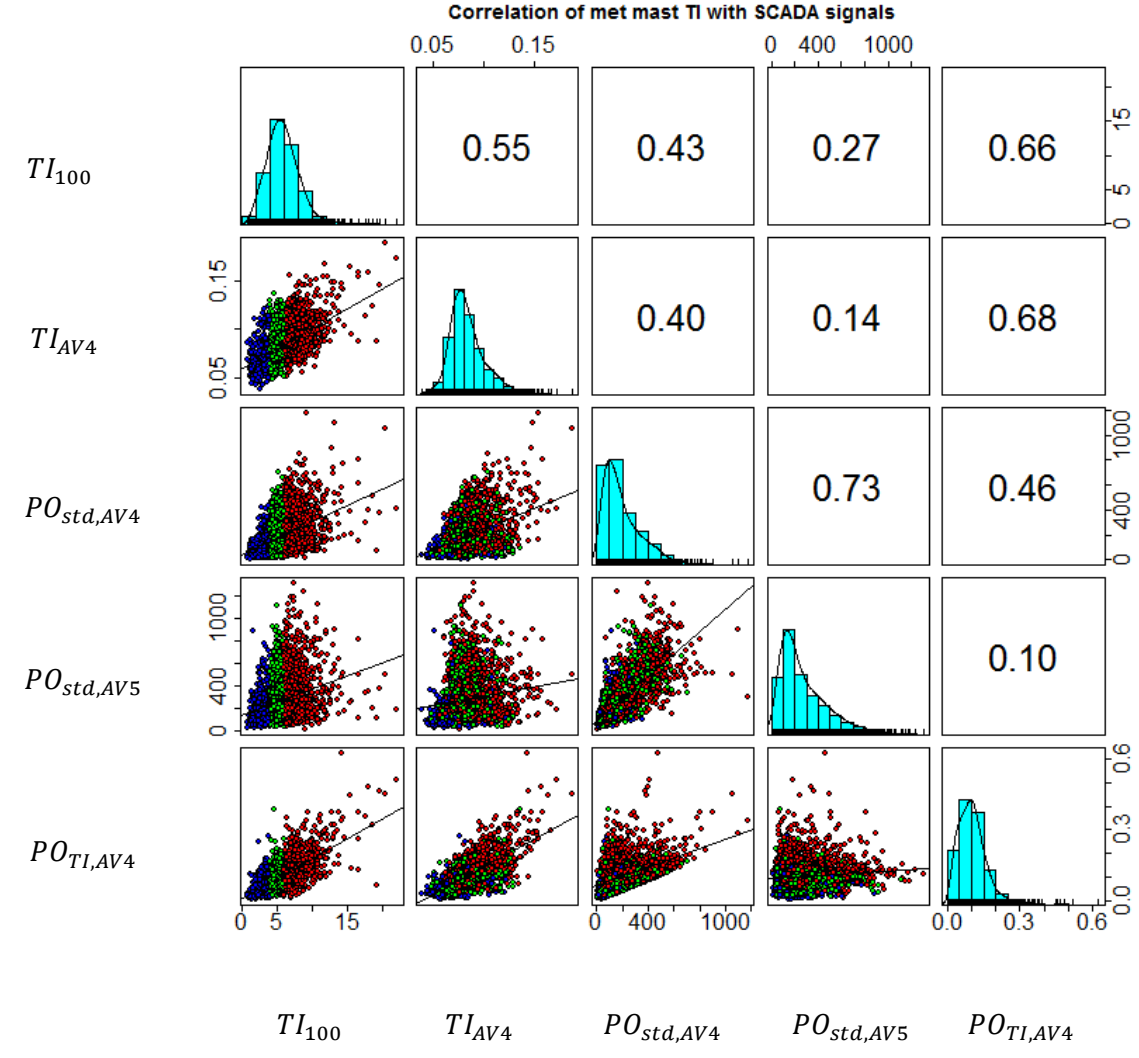

Figure 7: Correlation matrix. Turbulence intensity from met mast (TI_{100}) is correlated with the TI measured with the nacelle anemometer of AV4 (TI_{AV4}), the standard deviation of the 10 min power of AV4 ($PO_{std,AV4}$), the standard deviation of the 10min power of AV5 ($PO_{std,AV5}$) and the standard deviation of the power divided by the average power of AV4 ($PO_{TI,AV4}$). All dimensions are in [%] except for the standard deviation of the power which is in [kW].

To check the validity of these results, we use data from Nordsee Ost (NO). Figure 8 provides the information corresponding to Fig. 7 but for a different turbine type, met mast and a different location in the North Sea.

The correlation reveals the best result for the $PO_{TI,NO47}$signal (0.62). TI_{NO47} derived from the nacelle cup anemometer gives 0.60 . The difference between these two signals is much smaller than in alpha ventus. A different blade design and the distinct turbine nacelle met mast layout might be the reason for this.

Wind Energ. Sci. Discuss., doi:10.5194/wes-2016-60, 2017
Manuscript under review for journal Wind Energ. Sci.
Published: 3 February 2017

eawe european academy of wind energy
Open Access WIND ENERGY SCIENCE DISCUSSIONS

Both correlation analyses show that the new artificial SCADA signal, derived from the standard deviation of the power divided by its average active power PO_{TI} is the most suitable among the selected signals to substitute a met mast TI_{mast} for our purpose. In the next section, we check the influence of this new signal on the estimated power production in the wake.

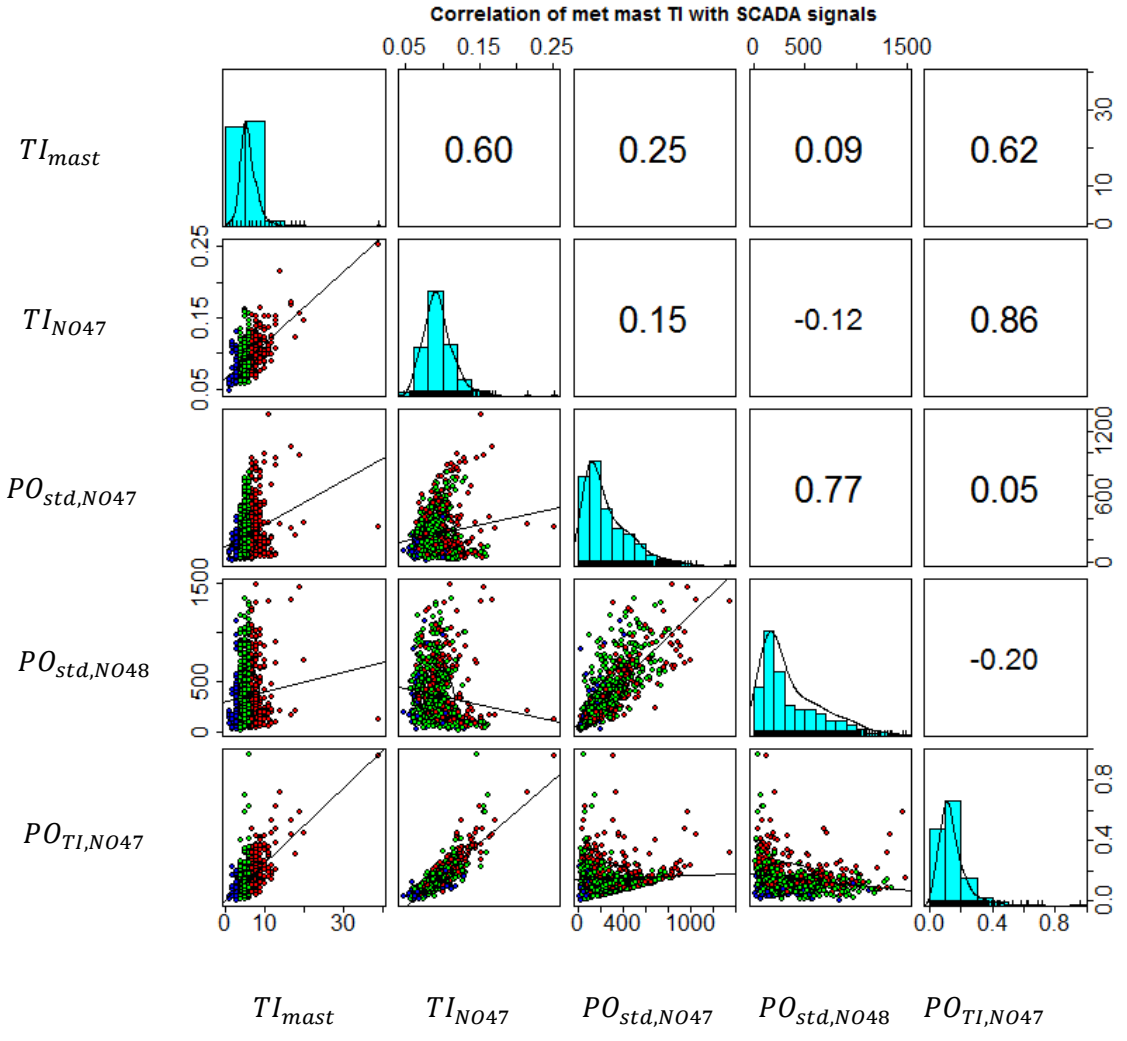

Figure 8: Correlation analysis for Nordsee Ost. Turbulence intensity (TI_{mast}) measured at hub height is correlated with the TI measured with the nacelle anemometer of NO47 (TI_{NO47}), the rotor estimated wind speed ($TI_{NO47_{u_{es}}}$), the standard deviation of the 10 min power of NO47 ($PO_{std,NO47}$), the standard deviation of the 10 min power of NO48 ($PO_{std,NO48}$), the standard deviation of the power divided by the average power of NO47 ($PO_{TI,NO47}$). All dimensions are in [%]except for the standard deviation of the power which is in [kW].

Wind Energ. Sci. Discuss., doi:10.5194/wes-2016-60, 2017
Manuscript under review for journal Wind Energ. Sci.
Published: 3 February 2017

eawe european academy of wind energy
Open Access WIND ENERGY SCIENCE DISCUSSIONS

4.3 New classification and validation

In Section 4.2 we demonstrated the correlation of the SCADA signal (PO_{TI}) derived by the standard deviation of the power divided by its average power with the turbulence intensity measured at a met mast in free flow conditions. In the next step, the ability of this signal to distinguish between different environmental stratification is analysed. Table 2 to Table 5 show the proposed thresholds for the different classifications for each wind farm (also corresponding to different turbine types).

4.3.1 alpha ventus (AV)

The classification of wake effects by the PO_{TI} signal is illustrated in Fig. 9 analogous to Fig. 5 where the turbulence intensity TI_{mast} is used.

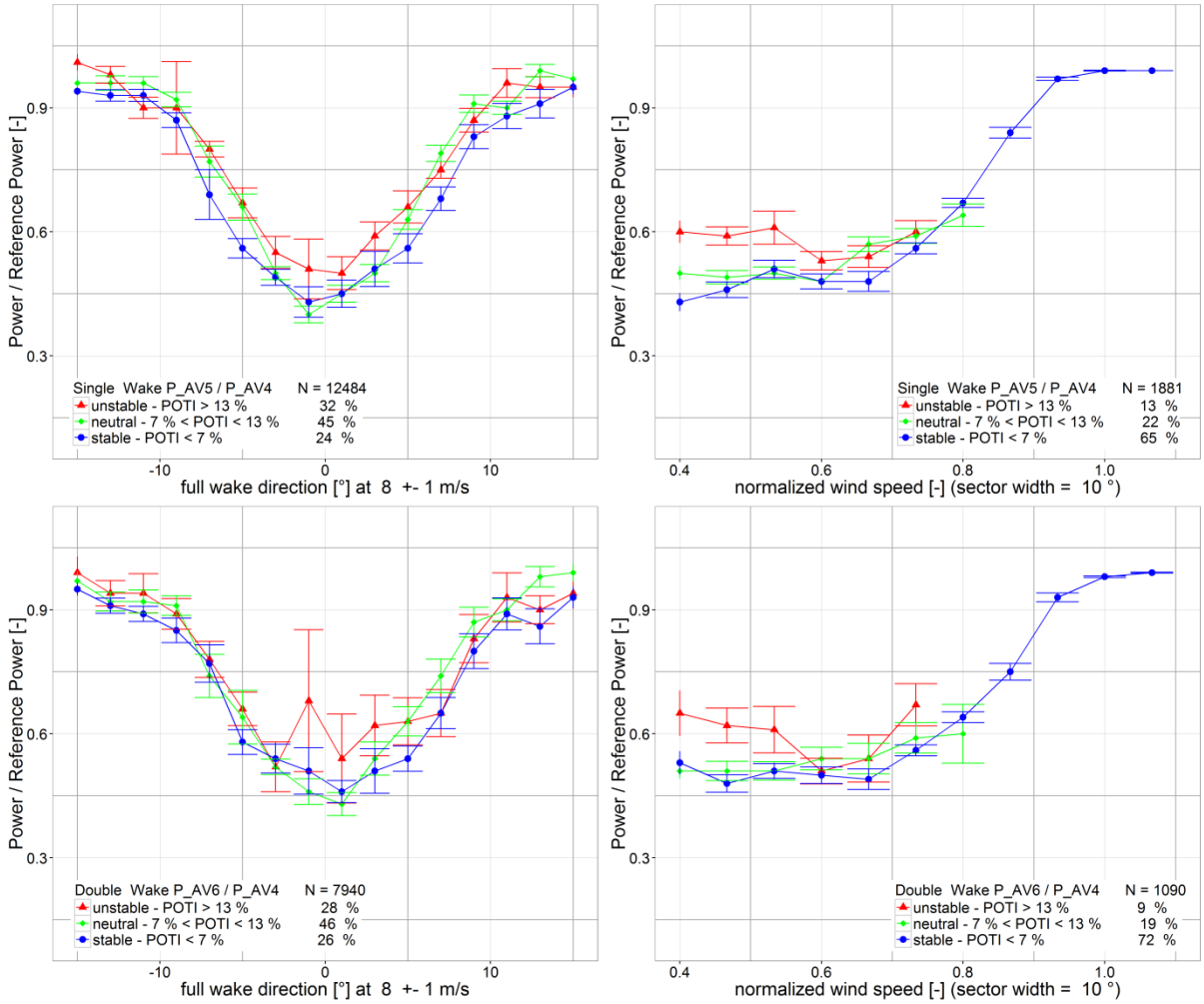

Figure 9: Stability classification with the PO_{TI} value. Power of waked turbine normalised with free flow turbine. Upper row: single wake, bottom row: double wake. Left column: Normalised Power as function of wind direction, right column: Normalised power as function of wind speed.

Wind Energ. Sci. Discuss., doi:10.5194/wes-2016-60, 2017
Manuscript under review for journal Wind Energ. Sci.
Published: 3 February 2017

eawe european academy of wind energy
Open Access WIND ENERGY SCIENCE DISCUSSIONS

A clear difference in power production between stable and unstable cases can be identified in the single wake. The differences in double wake are again less pronounced. Compared to the TI classification, the curves for the neutral case are not as clear as in-between the stable and unstable curves and in the normalized power curve plots (right column) the stable conditions can only be highlighted up to the wind speed of rated power for the free flow turbine. This can be explained with the fact, that at rated power the pitch controller rather than the power variation is governing the turbine reaction on turbulence intensity. This leads in Eq. (4) to a significant decrease of the numerator and keeps the denominator constant.

Table 2: Definition of stratification by power intensity: alpha ventus

Classification	Power Intensity (PO_{TI})
Unstable	$PO_{TI} > 13\ \%$
Neutral	$13\ \% \geq PO_{TI} \geq 7\ \%$
Stable	$7\ \% > PO_{TI}$

4.3.2 Nordsee Ost (NO)

The classification of wake effects in Fig. 10 is based on PO_{TI} and analogous to Fig. 6 where turbulence intensity TI_{mast} has been used. For these plots the Gaussian fitted minima's of the normalized wind speed (wake centres) measured by the LiDAR are plotted for each distance behind NO48.

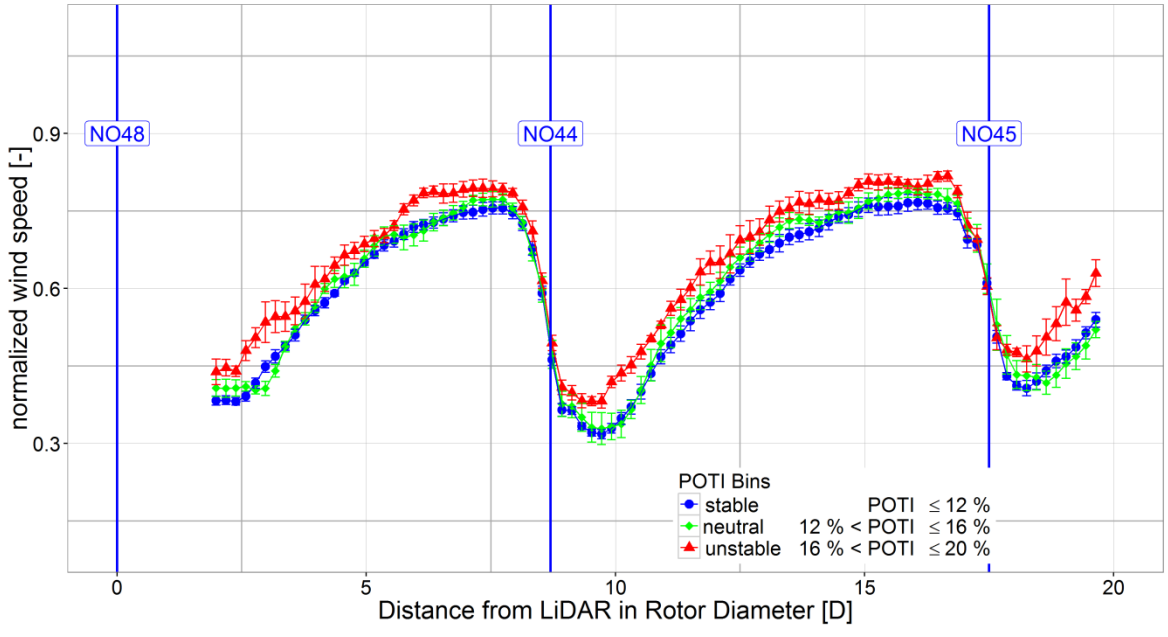

Figure 10: Wind speed recovery behind NO48 for different PO_{TI} classes. The wind speed is normalized with the inflow wind speed and the distance from the LiDAR on NO48 downstream is displayed in multiples of rotor diameters.

Again, this result states stronger wake effects for stable cases compared to unstable situations. The single wake has a less pronounced difference between the three classes and the slope of the wind speed recovery is smaller than the double wake case. E.g. 5D behind the first turbine, the wind speed has recovered to approximately 70% of the free flow wind speed and in

Wind Energ. Sci. Discuss., doi:10.5194/wes-2016-60, 2017
Manuscript under review for journal Wind Energ. Sci.
Published: 3 February 2017

the second wake 5D behind NO44 we see already more than 75%. This fact leads to the performance increase at the third turbine (NO45) compared to the second turbine (NO44). Wake added turbulence of NO48 is helping to recover the wind speed.

Table 3: Definition of stratification by power intensity: Nordsee Ost

Classification	Power Intensity (PO_{TI})
Unstable	$PO_{TI} > 16\ \%$
Neutral	$16\ \% \geq PO_{TI} \geq 12\ \%$
Stable	$12\ \% > PO_{TI}$

4.3.3 Ormonde (OR)

Finally the transferability of classification boundaries to other wind farms where no met mast is available is of interest.

First we have a look at the sensitivity of the proposed signal PO_{TI} in terms of turbulence from neighbouring turbines and wind farms. In Fig. 11, the directional bin averaged PO_{TI} from OR24 is able to identify the location of its neighbours. The magnitude allows to determine which turbine is next (OR25 at 4.2D) and which is further away (OR22 at 6.7D, OR23 at 6.6D and OR21 at 9.1D).

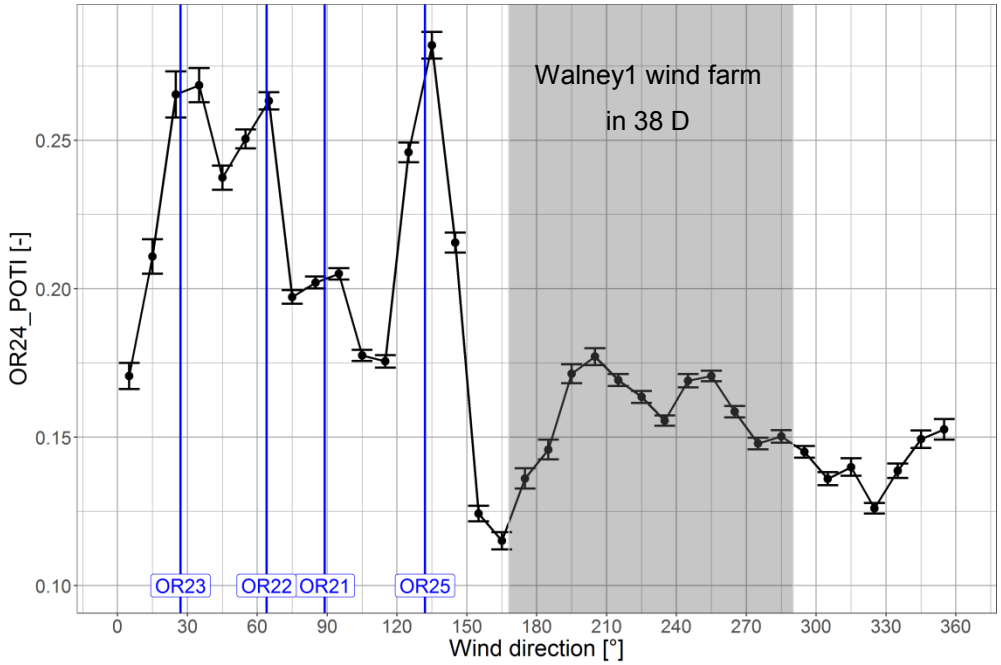

Figure 11: The new proposed signal PO_{TI} is sensitive to wake-induced turbulence from neighbouring turbines and wind farms. With PO_{TI} from turbine OR24 it is even possible to rank the distance of the neighbours being OR25 the closest with 4.2D and OR21 the farthest with 9.1D.

The grey area represents the geometrical location of the neighbouring wind farms Walney 1 and 2. The closest distance to OR24 has Walney 1 with approximately 38.8D (SWT-3.6-107 Siemens). The two peaks at 208° and 255° are wind directions

Wind Energ. Sci. Discuss., doi:10.5194/wes-2016-60, 2017
Manuscript under review for journal Wind Energ. Sci.
Published: 3 February 2017

for which multiple turbines of the neighbouring wind farm are aligned in a clear row of full wake situations. The increase from 345° to 15° can be explained with the coastline that gets quickly closer in clockwise direction.

Secondly we have a look at the influence on the wake recovery. With south westerly wind direction, we focus on single wake, double wake and triple wake conditions behind turbine number OR27 for a sector of 10° around the full wake situation. And for north westerly wind directions we investigate the rows of turbines behind OR23. The main differences between these two directions are the average level of inflow turbulence intensity and the different spacing between the turbines. In Fig. 11, the inflow turbulence level from north west (sector of 302 ° to 322 °) is much lower (bin average $\overline{PO_{TI}} \approx 12.5\ \%$) than from south west (sector of 192 ° to 222 °, bin average $\overline{PO_{TI}} \approx 17.5\ \%$) due to the wake effects from Walney 1 in more than 38D distance.

It was not possible to use exactly the same thresholds for the classification which is on the one hand a result of the usage of different turbines and controller versions in alpha ventus, Nordsee Ost and Ormonde. On the other hand there seems to be a dependence on the ambient turbulence level. Table 4 and Table 5 provides the new thresholds for the different classifications in Ormonde, estimated as described in Section 3.3.

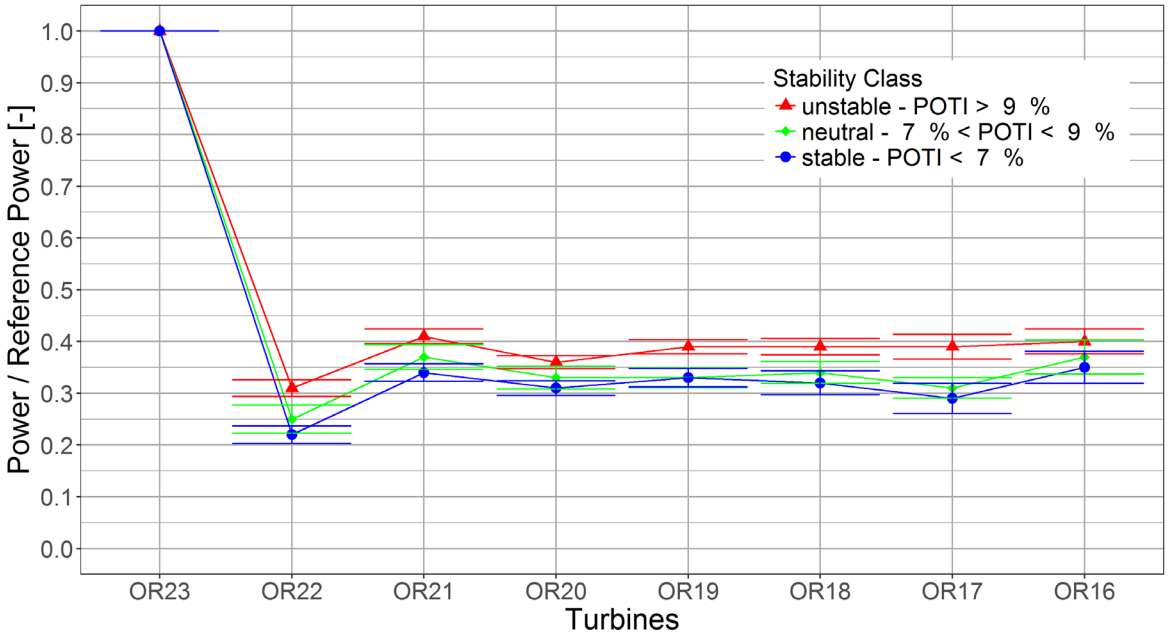

Figure 12: Normalized power for each turbine along the row behind OR23 for a wind direction of 312 ° and a 10 ° sector width and 8 m/s ±1. Stability classes distinguished with the signal PO_{TI} from OR23.

For north westerly wind direction, Fig. 12 provides a view on different wake effects at different stability classes. The normalized power for each turbine in the row behind OR23 is displayed (wind from left to right). Wind speed is filtered for 7 - 9 m/s and the wind direction is 312 ° with a sector width of 10 °. The largest wake effects are detected at OR22. This underlines the observation from the LiDAR measurements in NO. The first wake is the strongest and all consecutive wakes

Wind Energ. Sci. Discuss., doi:10.5194/wes-2016-60, 2017
Manuscript under review for journal Wind Energ. Sci.
Published: 3 February 2017

are better mixed due to wake added turbulence. The difference in power production between stable and unstable cases is in the range of 10%, which also demonstrates the importance of this effect for wake model developers to take it into account.

The south westerly wind direction is analyzed in Fig. 13, which is a similar illustration as Fig. 5 and Fig. 9. The PO_{TI} signal is on a higher level due to the wind farm wake effects from Walney 1 and 2. It is still possible to identify different wake behaviour for the different classes but the effect is less pronounced than in the previous examples. A higher level of inflow turbulence intensity contributes to the mixing of the wake with free wind. Hence at lower inflow turbulence levels the effect of the wake added turbulence is larger.

Further investigations are necessary to account for controller properties and to fill the normalized wind speed range [0.75 – 1], beyond the rated wind speed of the turbine in free flow conditions.

Table 4: Definition of stratification by power intensity: Ormonde for south westerly winds

Classification	Power Intensity (PO_{TI})
Unstable	$PO_{TI} > 18\ \%$
Neutral	$18\ \% \geq PO_{TI} \geq 13\ \%$
Stable	$13\ \% > PO_{TI}$

Table 5: Definition of stratification by power intensity: Ormonde for north westerly winds

Classification	Power Intensity (PO_{TI})
Unstable	$PO_{TI} > 9\ \%$
Neutral	$9\ \% \geq PO_{TI} \geq 7\ \%$
Stable	$7\ \% > PO_{TI}$

In performance monitoring of offshore wind farms the newly aggregated SCADA signals can be used as an auxiliary quantity to classify different atmospheric stability conditions. Advanced engineering wake models which are able to take turbulence intensity or stability parameters into account, may be parameterized by these artificial turbine signals in order to improve their prediction of wind turbine power production under waked conditions.

Wind Energ. Sci. Discuss., doi:10.5194/wes-2016-60, 2017
Manuscript under review for journal Wind Energ. Sci.
Published: 3 February 2017

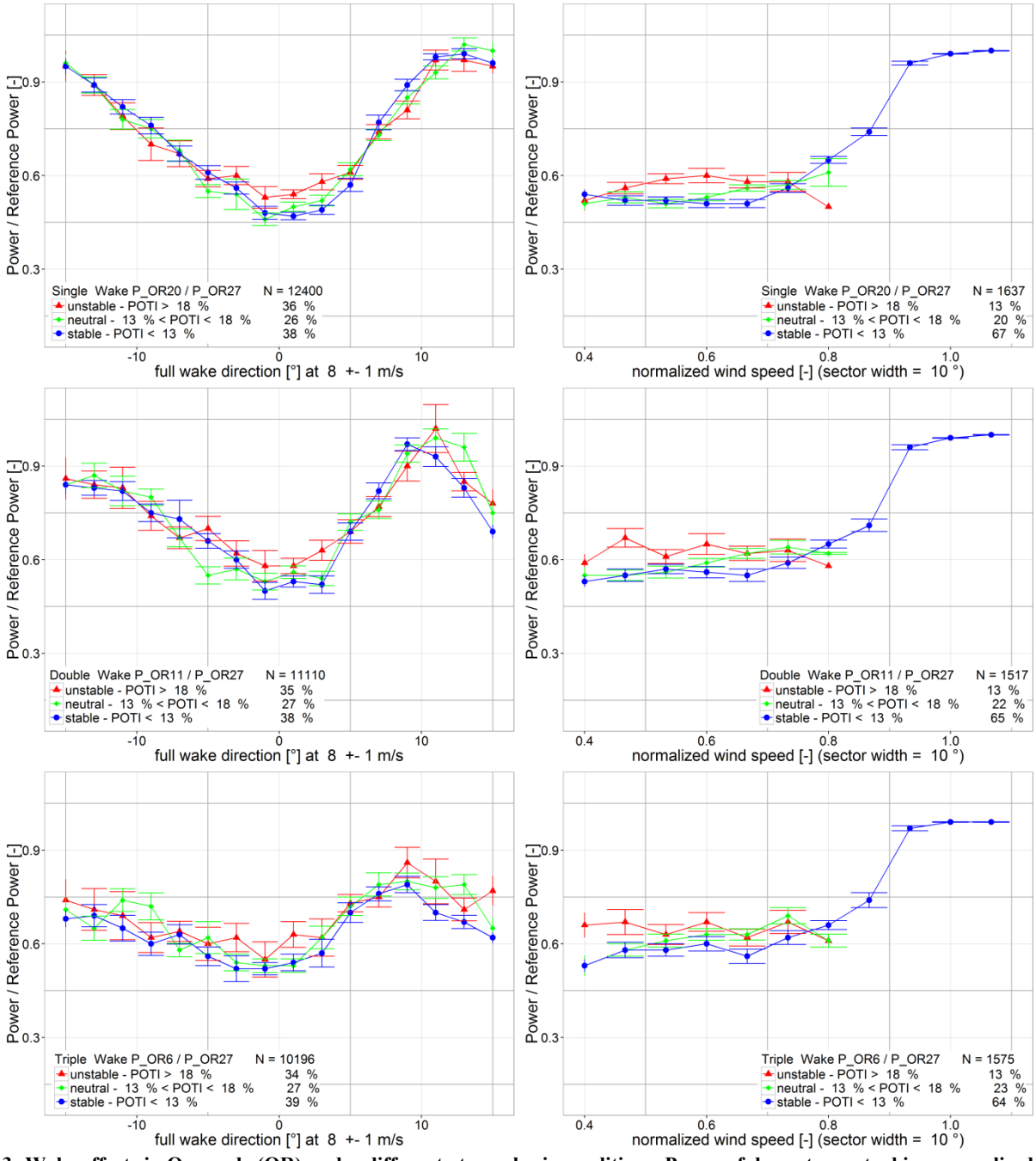

Figure 13: Wake effects in Ormonde (OR) under different atmospheric conditions. Power of downstream turbine normalised with free flow turbine. First row: single wake, second row: double wake and third row: triple wake. Left column: Normalised Power as function of wind direction, right column: Normalised power as function of wind speed.

Wind Energ. Sci. Discuss., doi:10.5194/wes-2016-60, 2017
Manuscript under review for journal Wind Energ. Sci.
Published: 3 February 2017

5 Conclusions

Measured data from three different offshore wind farms, two met masts and one long range LiDAR has been analysed to identify different influence on power production at turbines operating in the wake. We have validated the method described in Dörenkämper (2015), which proposes to use the turbulence intensity, to describe the power production in the wake. A correlation analysis was performed and for wind speeds in partial load operation, the standard deviation of the power divided by its average power (PO_{TI}) was identified having similar behaviour than the turbulence intensity. A sensitivity check for PO_{TI} reviled very detailed responsiveness to increases in turbulences due to neighbouring turbines and wind farms. Effects from wind farm neighbours are detectable even more than 38 rotor diameter away. A classification of different turbine behaviour based on PO_{TI} was analysed and compared to the classification with turbulence intensity TI.

Both signals can distinguish between stronger and weaker wake effects. A transferability of the findings from one turbine to the next is only possible under the prerequisite of having the same turbine type and controller version. The magnitude of influence of the PO_{TI} signals on wake effects is dependent on the level of inflow turbulence intensity. Higher inflow turbulence has already a higher wake mixing and therefore the wake added turbulence has a less pronounced contribution.

Using PO_{TI} to predict wakes more accurate is a promising approach, but further investigations are necessary to take controller properties into account and to fill the wind speed range beyond the rated wind speed.

Acknowledgements

The presented work is partly funded by the Commission of the European Communities, Research Directorate-General within the scope of the project “ClusterDesign” (Project No. 283145 (FP7 Energy)). We would like to thank Deutsche Offshore-Testfeld und Infrastruktur GmbH & Co. KG (DOTI), Research at alpha ventus (RAVE), Innogy SE, Vattenfall Wind Power and Senvion SE for making this investigation possible. Furthermore a special thanks to the R Core Team for developing the open source language R (R_Core_Team, 2015).

References

Beck, H., Trabucchi, D., Bitter, M. and Kühn, M.: The Ainslie Wake Model An Update for Multi Megawatt Turbines based on State-of-the-Art Wake Scanning Techniques, in Proceedings of the European Wind Energy Association, Barcelona, Spain, 10-13 March., 2014.

Dörenkämper, M.: An investigation of the atmospheric influence on spatial and temporal power fluctuations in offshore wind farms, PhD Thesis, University of Oldenburg, Oldenburg., 2015.

Dörenkämper, M., Tambke, J., Steinfeld, G., Heinemann, D. and Kühn, M.: Influence of marine boundary layer

characteristics on power curves of multi megawatt offshore wind turbines, in Proceedings of 11th German Wind Energy Conference, Bremen, Germany, 7-8 November., 2012.

Göçmen, T. and Giebel, G.: Estimation of turbulence intensity using rotor effective wind speed in Lillgrund and Horns Rev-I offshore wind farms, Renew. Energy, 99, 524–532, doi:10.1016/j.renene.2016.07.038, 2016.

Hamilton, N.: Functions Relating to the Smoothing of Numerical Data, CRAN R, 1–5, 2015.

Iungo, G. V. and Porté-Agel, F.: Volumetric scans of wind turbine wakes performed with three simultaneous wind LiDARs under different atmospheric stability regimes, J. Phys. Conf. Ser., 524, 12164, doi:10.1088/1742-6596/524/1/012164, 2014.

Keane, A., Aguirre, P. E. O., Ferchland, H., Clive, P. and Gallacher, D.: An analytical model for a full wind turbine wake, J. Phys. Conf. Ser., 753(3), 32039 [online] Available from: http://stacks.iop.org/1742-6596/753/i=3/a=032039, 2016.

Mittelmeier, N., Blodau, T. and Kühn, M.: Monitoring offshore wind farm power performance with SCADA data and advanced wake model, Wind Energy Sci. Discuss., 2016, 1–25, doi:10.5194/wes-2016-16, 2016.

More, G. and Gallacher, D.: Lidar Measurements and Visualisation of Turbulence and Wake Decay Length, in Proceedings of the European Wind Energy Association, Barcelona, Spain, 10-13 March., 2014.

Mortensen, N. G., Nielsen, M. and Ejsing Jørgensen, H.: Offshore CREYAP Part 2 – final results, European Wind Energy Association (EWEA), Helsinki, Finland, 2.Juni 2015., 2015.

Ott, S. and Nielsen, M.: Developments of the offshore wind turbine wake model Fuga, E-0046 Report 2014, DTU Wind Energy, Lyngby, Denmark., 2014.

Özdemir, H., Versteeg, M. C. and Brand, A. J.: Improvements in ECN Wake Model, in Proceedings of the ICOWES2013 Conference, Lyngby, Denmark, 17-19 June., 2013.

R_Core_Team: R: A Language and Environment for Statistical Computing, [online] Available from: https://www.r-project.org/, 2015.

Saint-Drenan, Y.-M., Hagemann, S., Lange, B. and Tambke, J.: Uncertainty in the vertical extrapolation of the wind speed due to the measurement accuracy of the temperature difference, in Proceedings of European Wind Energy Conference, EWEC, Marseille, France, 16-19 March., 2009.

Schneemann, J., Trabucchi, D., Trujillo, J. J. and Voß, S.: Long range scanning lidar measurement campaign report, ClusterDesign Deliverable 7.1, ClusterDesign, Project No. 283145 (FP7 Energy)., 2016.

Tuerk, M.: Ermittlung designrelevanter Belastungsparameter für Offshore-Windkraftanlagen, PhD Thesis, Universität zu Köln., 2008.

Vollmer, L., Steinfeld, G., Heinemann, D. and Kühn, M.: Estimating the wake deflection downstream of a wind turbine in different atmospheric stabilities: An LES study, Wind Energ. Sci, 1, 129–141, doi:10.5194/wes-1-129-2016, 2016.

Westerhellweg, A., Cañadillas, B., Kinder, F. and Neumann, T.: Wake Measurements at alpha ventus – Dependency on Stability and Turbulence Intensity, J. Phys. Conf. Ser., 555(1), 12106, 2014.